DOI: 10.1002/ejic.200800899

Biomimetic Modelling of Copper Enzymes: Synthesis, Characterization, EPR Analysis and Enantioselective Catalytic Oxidations by a New Chiral Trinuclear Copper(II) Complex

Francesco G. Mutti,[a] Giorgio Zoppellaro,[b] Michele Gullotti,*[a] Laura Santagostini,[a] Roberto Pagliarin,[c] K. Kristoffer Andersson,[b] and Luigi Casella[d]

Keywords: Copper / Ligand effects / EPR spectroscopy / Oxidation / Enzyme models

The new octadentate ligand (*R*)-(+)-*N*,*N*′-dimethyl-*N*,*N*′-bis{-2-[bis(1-methyl-2-benzimidazolylmethyl)]-2-methylaminoethyl}-1,1′-binaphthyl-2,2′diamine [(*R*)-(+)-DABN-L-Ala-Bz_4; L] was employed for the synthesis of dinuclear and trinuclear copper(II) complexes. The ligand design is based on the insertion of chiral residues derived from L-alanine between the diaminobinaphthyl (*R*)-(+)-DABN spacer and the aminobis(benzimidazole) metal binding units. The chiroptical properties of the ligand and the complexes are described. EPR experiments were performed on $[Cu_2L]^{4+}$ and $[Cu_3L]^{6+}$ at low temperatures. In the case of $[Cu_2L]^{4+}$, a weak dipolar interaction between the two spin centres was found. A similar weak spin interaction occurred in the trinuclear copper cluster, which could be treated likewise as a weakly coupled three-spin system. The analysis was substantiated by studying the complex EPR temperature behaviour, where population of the quartet state occurred only at high temperature (77 K), whereas at cryogenic temperatures (4 K) the system adopted a doublet state as a ground-state spin configuration. Titration with sodium azide of $[Cu_2L]^{4+}$ was consistent with terminal binding of one N_3^- molecule to each copper ion. Furthermore, dipolar interactions between spin centres were strongly suppressed in this case. For $[Cu_3L]^{6+}$, the adduct formed by the interaction with two azido molecules induced formation of a μ-azido bridges among the three Cu^{2+} ions and led to population of the quartet state even at cryogenic temperatures. This bridged configuration was, however, lost upon further addition of azido molecules. The copper(II) complexes were tested as catalysts in the oxidation of biogenic catechols and flavonoids by dioxygen to give the corresponding quinones, which were trapped as adducts with MBTH. The dinuclear complex $[Cu_2L]^{4+}$ displays poor substrate enantiodifferentiating ability, even though it exhibits catalytic activity comparable to that of $[Cu_3L]^{6+}$. The trinuclear complex $[Cu_3L]^{6+}$ exhibits significant enantioselectivity in the oxidations of the catecholamines L-/D-dopa methyl ester and L-/D-norepinephrine. The origin of this enantioselectivity must be associated with the mode of substrate binding, as it depends almost entirely on K_M.

Introduction

The area of bioinorganic chemistry continues to expand its interest towards different disciplines.[1] Many different strategies involving macrocyclic and nonmacrocyclic systems have been developed for the construction of ligands containing multiple reaction sites. A major goal of this work lies in the generation of enzyme-like properties, with rate acceleration and reaction specificity.[2] We expect that the future of synthetic modelling of metal enzymes will involve functional and catalytic models capable of reproducing or approaching biological reactivity. The synthetic variability of the ligands coupled with the ability to examine reactions at such fine detail provides an approach to dissect biological reactivity that is complementary to studies of the enzymes. Over the past decade, chemists have designed numerous artificial systems based on metal–ligand coordination that provide, for example, many elegant studies of selective and environmentally benign oxidants capable of performing interesting organic transformations, and many of these are copper complexes that use molecular oxygen as the ultimate oxidant.[3] Chirality is a fundamental feature that pervades the living world, and the preference for one enantiomer over the other is a peculiar feature of the biological systems. Various biomolecules utilize a large number of sophisticated chemical interactions to direct the assembly of higher-ordered multicomponent systems that retain the structural and stereochemical nature of the subunits. Chiral

[a] Dipartimento di Chimica Inorganica, Metallorganica e Analitica "Lamberto Malatesta", Università di Milano, Istituto ISTM-CNR,
Via Venezian 21, 20133 Milano, Italy
Fax: +390250314405
E-mail: michele.gullotti@unimi.it
[b] Department of Molecular Biosciences, University of Oslo, N0316 Oslo, Norway
[c] Dipartimento di Chimica Organica e Industriale, Università di Milano,
Via Venezian 21, 20133 Milano, Italy
[d] Dipartimento di Chimica Generale,
Via Taramelli 12, 27100 Pavia, Italy

coordination complexes find applications in enantioselective synthesis, in asymmetric catalysis, as nonlinear optical materials or even as novel magnetic materials.[4] Our previous work focused on the construction of chiral multinuclear biomimetic complexes with the hope of utilizing the enzyme-like properties and functionalities for enantioselective processes.[5] The first trinuclear copper complex derived from an octadentate nitrogen ligand containing two chiral L-histidine residues as chelating arms connected to a central piperazine spacer[5a] proved to be capable of performing the catalytic oxidation of chiral catechols to quinones with remarkable enantiodifferentiation,[5b] and it also possessed phenol monooxygenase activity.[6] Subsequently, other trinuclear copper complexes were derived from ligands with different design, where the chiral moiety was contained in a central 1,1-binaphthyl spacer, to which two nonchiral chelating arms were attached.[7] Also, these complexes performed, with different recognition mechanisms, enantioselective catalytic oxidations of chiral catechols. In this paper we wish to describe the synthesis and the complete spectroscopic, magnetic and conformational characterization of the dinuclear and trinuclear copper(II) complexes derived from a new chiral ligand, namely (*R*)-(+)-DABN-L-Ala-Bz_4 (L), which improves the previously studied systems in that it contains chiral centres both in the central (1,1′-binaphthyl) spacer and in the side arms. The catalytic oxidase activity of these complexes towards chiral substrates was also investigated to ascertain whether the three chiral centres favourably concur to increase the enantioselectivity of the processes.

Results and Discussion

Synthesis of the Ligand and the Copper Complexes

The schematic representation of the (*R*)-(+)-DABN-L-Ala-Bz_4 ligand is depicted in Scheme 1. The diamine (*R*)-(+)-DABN was condensed with the protected amino acid *Z*-L-Ala-OH to give compound **2** that was deprotected, by reduction, to compound **3**. Compound **3** was treated in DMF solution and in the presence of anhydrous sodium carbonate with an excess of 2-chloromethyl-1-methylbenzimidazole to afford **4**. *N*-methylation of compound **4** (diamide bonds) with NaH and MeI gave intermediate **5**, and finally, reduction of the carbonyl groups with $BH_3{\cdot}Me_2S$ in tetrahydrofuran solution led to the ligand (*R*)-(+)-DABN-L-Ala-Bz_4 (L). The intermediate compounds of all the reactions carried out to obtain ligand L must undergo several purifications steps, because the product mixtures showed the presence of several byproducts and unreacted reagents even after long reaction times. The overall intermediates were completely characterized by chemical analyses and ^1H NMR, ^{13}C NMR, ESI-MS, UV/Vis and CD techniques. The ESI-MS spectra of all the compounds are in good agreement with the simulated spectra together with additional clusters of peaks corresponding to the adducts with a sodium ion, which is always present in the medium. The copper(II) complexes $[Cu_2L](ClO_4)_4$ and $[Cu_3L](ClO_4)_6$ were isolated by treating two or three molar equivalents of copper(II) perchlorate, respectively, with a solution of the ligand in MeCN, at room temperature for the dinuclear complex, and at reflux for 2 d, for the trinuclear complex. The resulting red-wine or brown solutions gave a red or violet precipitate of $[Cu_2L](ClO_4)_4$ or $[Cu_3L](ClO_4)_6$, respectively, upon addition of diethyl ether. In principle, on

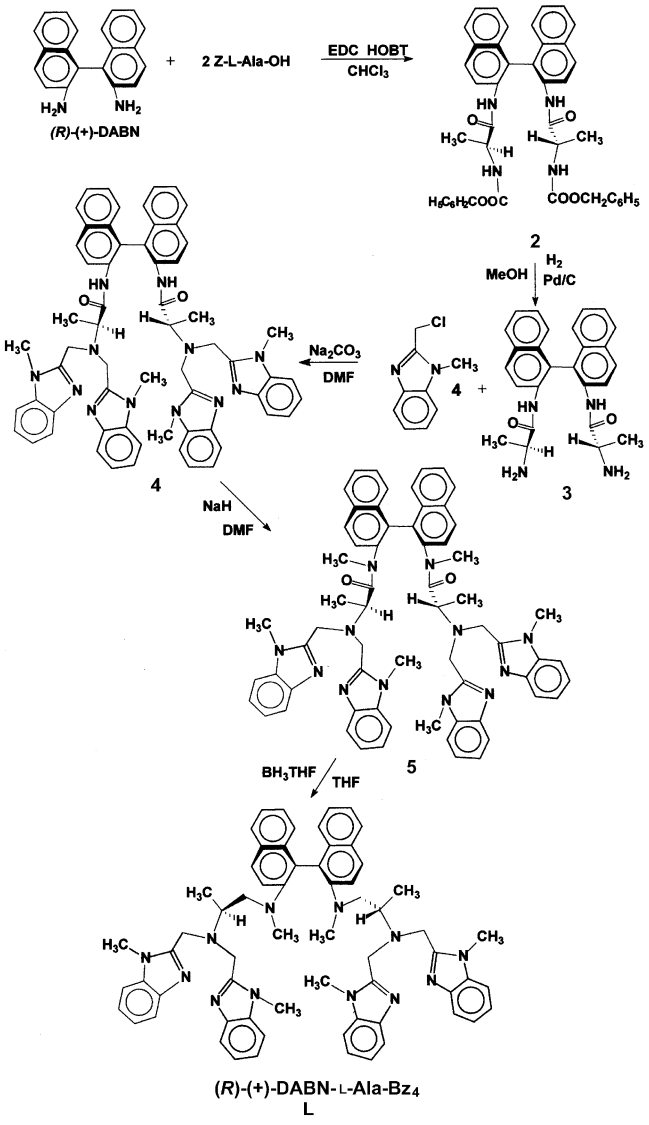

Scheme 1. Synthetic route for the preparation of the (*R*)-(+)-DABN-L-Ala-Bz_4 ligand.

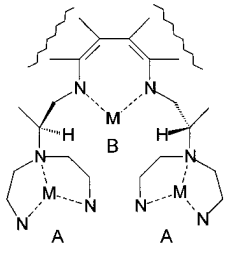

Scheme 2. Schematic representation of the distribution of the Cu centres in the trinuclear complex.

the basis of the results obtained for the dinuclear and trinuclear complexes with octadentate ligands of the same family,[7] we expect that the two copper ions in the $[Cu_2L]^{4+}$ cation should bind to the tridentate aminobis(benzimidazole) residues (A sites),[7d] whereas in $[Cu_3L]^{6+}$ the two copper ions should be located at the tridentate A sites and the third copper ion to the bidentate nitrogen donors of the diaminobinaphthyl group (B site) (see Scheme 2).

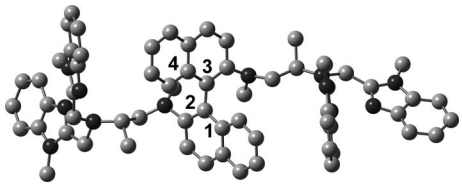

Figure 1. Optimized geometry (PM3MM) for the (*R*)-(+)-DABN-L-Ala-Bz_4 ligand. Hydrogen atoms are not depicted for clarity. Carbon atoms are depicted in light grey and nitrogen atoms in dark grey. The resulting torsion angle (C1–C2–C3–C4) between the two naphthyl groups is $|\theta| = 103.0°$.

Spectroscopic Properties

The electronic spectrum of L recorded in MeCN solution exhibits transitions associated with both the 1,1′-binaphthyl and benzimidazole chromophores. Thus, as already reported for other binaphthyl-derived ligands,[7a,7d] the former chromophore is mostly responsible for the absorptions at 255 and 306 nm, and the latter for the multicomponent bands at 271, 278, 285 nm, whereas both chromophores contribute to the bands at 255 and 361 nm. The CD pattern of L closely resembles that observed for other 1,1′-binaphthyl-derived chiral ligands,[7a,7d] showing that the amino acids bonded to the 1,1′-binaphthyl residue do not alter the chiroptical properties of the chromophore. The spectrum consists of a weak negative Cotton effect at 370 nm flanked at higher energy by two dichroic bands at 293 (positive) and 257 nm (negative) and by a rather intense exciton doublet featuring a negative peak at 225 nm and a positive peak at 211 nm. However, there are two important differences among (*R*)-(+)-DABN-L-Ala-Bz_4 and the other 1,1′-binaphthyl-derived ligands: the CD couplet of the former compound is in fact of lower intensity and, furthermore, the spectrum lacks the distinctive CD feature at 248 nm,[7b] indicating that this ligand is unable to maintain stacking interactions between the naphthyl rings and the benzimidazole groups in the side arms, as for the other ligands, and therefore, the conformational arrangement of the naphthalene ring should correspond to poorly strained 1,1′-binaphthyl chromophores, which typically involves dihedral angles not far from 90°.[7b,8] This is shown in Figure 1 by modelling the ligand through quantum chemical calculation (semiempirical method, PM3MM). Although the system is characterized by a large degree of freedom due to the presence of several N and C sp^3 (σ) bonds, the optimized structure reveals a *transoid* conformation characterizing the naphthyl chromophores, with $|\theta| = 103.0°$. This dihedral angle is almost identical to that observed in the crystalline A form (chiral) of 1,1′-binaphthyl ($\theta = 103.1°$).[9]

The near-UV CD couplet of the 1,1′-binaphthyl chromophore is completely absent in the spectra of the dinuclear and trinuclear complexes, which contain only a weak positive CD band at 217 nm. This indicates that coordination of Cu^{II} ions to L imposes a marked flattening of the dihedral angle between the naphthalene planes due to the coordination requirement of the Cu^{II} ions that tend to arrange the ligand nitrogen donors in a nearly coplanar disposition. The optical activity of the copper complexes in the low-energy range of the spectrum is rather weak, even though the CD spectrum of the trinuclear complex is richer than that of the parent dinuclear complex. As the chiral centres of the L-alanine arms are outside the chelating rings of the Cu^{II} ions in the A sites, their (vicinal) effects on the Cu d–d transitions are small, and also the flattening of the 1,1′-binaphthyl chromophore contributes to make CD induction into the transitions of the Cu^{II} ion in the B site extremely weak, as it also occurred with other 1,1′-binaphthyl-derived trinuclear complexes described before.[7c] It is worth noting that, particularly for $[Cu_3L]^{6+}$, the near-UV optical spectrum contains electronic bands of sizeable intensity in the range between 300 and 400 nm, which may be related to hydroxido to Cu^{II} LMCT transitions, where the hydroxido groups are originated by dissociation of Cu-bound water molecules.[10b,11]

Binding of Azido Ligands to the Copper Complexes

Binding of azido ligands to copper(II) centres is generally accompanied by the appearance of LMCT transitions in the near-UV and visible region that result in moderately intense absorption bands in the range between 350 and 500 nm. Spectral titration of the $[Cu_2L]^{4+}$ complex shows a symmetrical band at 396 nm as the azido anion is added, and it is noteworthy that from the intensity increase it can be deduced that only two azido ligands can bind to the complex,[10,11] as even at high concentration of the ligand the LMCT band maintains the same intensity. On the basis of previous studies,[10a,10b] the symmetric shape of the LMCT band confirms that the adduct contains two terminal azido ligands. However, it is impossible to estimate the values of the binding constants for azido association to the Cu^{II} ions, because no isosbestic points were evident in the spectra.

The azido binding experiments on $[Cu_3L]^{6+}$ display somewhat unusual behaviour in that the spectrum of the complex undergoes no marked changes up to a ratio of $[N_3^-]/[Cu_3] \approx 1:1$; only a weak and broad band around 370–380 nm develops in solution. This behaviour suggests that the trinuclear compound is in a closed conformation, possibly maintained by hydroxide bridging ligand(s) between the metal ions, as suggested by the optical spectrum described above, which hinders the binding of the azido ligands. Addition of an additional azido unit to a ratio of $[N_3^-]/[Cu_3] \approx 2:1$ produces the development of a two-component band

with maximum at 395 nm and a shoulder at ≈340 nm, indicating that the two azido ligands are bridging the copper ions (likely in a μ-1,3 mode) and, hence, also stabilize a folded configuration for the $[Cu_3L]^{6+}$ complex. Upon further addition of azido ligands, up to a ratio of $[N_3^-]/[Cu_3] \approx 3:1$, the two components merge into a single symmetric band at 400 nm, which suggests that cleavage of the existing μ-1,3 bridges occurs, producing an adduct with azido molecules bound end on. Unfortunately, also in this case, the absence of isosbestic points during the titration precludes the determination of binding constants.

EPR Experiments and Analysis

The EPR spectrum of the $[Cu_2L]^{4+}$ complex recorded in diluted glassy solution at cryogenic temperature (T = 4 K) is shown in Figure 2. It exhibits a poorly resolved pattern for the Δm_s = 1 transition with spin-Hamiltonian parameters consistent with Cu^{II} ions in a distorted square pyramidal structure and with $g_{\parallel}$ = 2.234, $g_{\perp}$ = 2.083 and $A_{\parallel}$ = 14.7 mT. However, close inspection of the spectrum reveals the forbidden half-field transition (Figure 2, inset; g_{av} = 4.2) and, hence, the presence of a species with a triplet-state configuration (S = 1) within the system. Furthermore, the Δm_s = 2 resonance is characterized by a resolved hyperfine term ($A_{\parallel}$ = 7.4 mT) that is roughly half of the copper hyperfine term ($A_{\parallel}$) observed in the Δm_s = 1 resonance line.

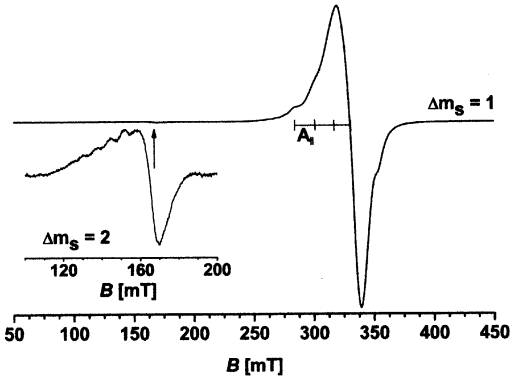

Figure 2. EPR spectra of $[Cu_2L]^{4+}$ (1.3 mM in MeCN/MeOH, 8:2). Instrumental parameters: frequency 9.664385 GHz, 100 kHz modulation frequency, 0.746 mT modulation amplitude, 80 μW microwave power, 168 s sweep time, 82 ms time constant, 5 scans, T = 4 K. The instrumental parameters for Δm_s = 2 transition were as follows: frequency 9.664365 GHz, 100 kHz modulation frequency, 0.746 mT modulation amplitude, 0.4 mW microwave power, 84 s sweep time, 82 ms time constant, 16 scans, T = 4 K.

Here the exchange term J between the two spin S = 1/2 centres needs to be larger than the isotropic Cu hyperfine term, $|J|>|A|$, but it can be as small as 0.02 cm^{-1}.[12] In the case of a dipolar coupled dinuclear complex, the transition probability for the Δm_s = 1 line depends on the value of both the exchange term, $J(S_1S_2)$, and the anisotropic exchange, whereas the half-field Δm_s = 2 transition depends only on the anisotropic exchange. As a consequence, often in weakly coupled systems this transition remains undetected.[13] The very low intensity of the Δm_s = 2 transition indicates the occurrence of a very small dipolar through-space interaction between the copper ions ($D << 9 \times 10^{-3}$ cm^{-1}), with dimer features remaining broadened and unresolved along Δm_s = 1. This is a very small ZFS term and the space proximity of the two copper centres must be much larger than 5 Å, which hence prevents the possibility that small ligands, such as water molecules or hydroxide ions, are bridging the two metal ions. The spin concentration accounts for S_c = 1.80 ± 0.10 spins against CuEDTA standard and remains almost constant up to the higher temperature range examined (T = 77 K, S_c = 1.85 ± 0.10 spins). No significant changes in the overall Δm_s = 1 resonance transition (shown in Figure 5A) is observed upon raising the temperature from T = 4 K to T = 77 K. Despite the fact that the forbidden half-field transition is completely undetected at T = 77 K, a small broad resonance at $g < 2$ still remains visible in the spectrum. Hence, the triplet species S = 1 represents only a very minor fraction of the dinuclear spin system, and thus, it is difficult to quantify its relative amount. We furthermore speculate that in this high-spin fraction (Cu dimer) a very small energy difference between the singlet and triplet states characterizes $[Cu_2L]^{4+}$; hence, they remain populated according to the Boltzmann distribution, at least down to 4 K. In this vein, the geometry optimization and theoretical analyses carried out on multinuclear copper complex[14] as well as for the catalytic active site in copper enzymes[15] provide additional information of the complex conformation and metals electronic structure. However, as pointed out in recent work,[16] there is no general method for the accurate computation of copper(II) complexes, and therefore, the choice of the method strongly depends on the ligand type and chromophore nature. As a result of the complexity of the present system, the theoretical modelling was obtained by the molecular mechanics (UFF) force field method, and the geometries around the metal ions were further optimized by density functional methods (UHF/DFT) with the aid of hybrid-exchange functional and the correlation functionals from Lee, Yang and Parr (B3LYP) and LanL2DZ basis set, assuming that the complex has a doublet as the ground-state spin multiplicity. As shown in Figure 6A, the two copper ions share identical coordination geometries (slightly distorted square pyramid). The nitrogen donors from one benzimidazole (N1) and the tertiary amino (N3) group together with two coordinated hydroxide molecules, which have been arbitrarily added for charge balancing, occupy the equatorial positions and the third nitrogen donor from the second benzimidazole residue (N2) occupies the axial position. The Cu–N computed distances are collected together in Figure 6A. The Cu–N bonds (benzimidazole rings) are shorter (1.93 Å) than those witnessed for Cu–N tertiary amino groups (2.14 Å). These values resemble well those observed in the X-ray structure analyses of other dinuclear copper complexes derived from a triaminopentabenzimidazole ligand[17] and a tetraaminotetrabenzimidazole ligand.[18] Furthermore, the computed Cu–N bonds for the benzimidazole rings are consistent with the distances known in copper chelates with imidazole/benzimidazole N-

donors in the equatorial/axial plane, which usually lie in the range 1.94–2.06 Å.[19] The torsion angle between the two naphthyl groups is slightly smaller ($|\theta| = 99°$) than the value calculated in the metal-free ligand. Because the optimized structure shows an intramolecular Cu1A–Cu2A distance of 11.6 Å, the through-space interaction between spin centres is negligible, in agreement with the EPR findings.

The EPR spectrum of the trinuclear complex $[Cu_3L]^{6+}$ recorded at cryogenic temperature (T = 4 K) is illustrated in Figure 3. Surprisingly, it closely resembles the spectrum of $[Cu_2L]^{4+}$, and it is more consistent with isolated Cu centres, even though a close proximity of the three Cu^{2+} ions is expected. However, small hyperfine resonances appear in the low field $\Delta m_s = 1$ region, around 260 mT, accompanied by the half-field transition (Figure 3, left inset, $g_{av} = 4.2$) indicative of the presence of triplet species, which also presents a resolved hyperfine structure ($A_{\|} = 6.7$ mT). This is a smaller hyperfine term than that previously witnessed in $[Cu_2L]^{4+}$ for the minor $S = 1$ species. The spin concentration accounts for $S_c = 1.96 \pm 0.10$ spins at 4 K against CuEDTA standard, which is much less than three uncorrelated spins and almost equal to two doublets (2 $S_{1/2}$). Upon increasing the temperature to 77 K, the amount of detected spin increases (Figure 4).

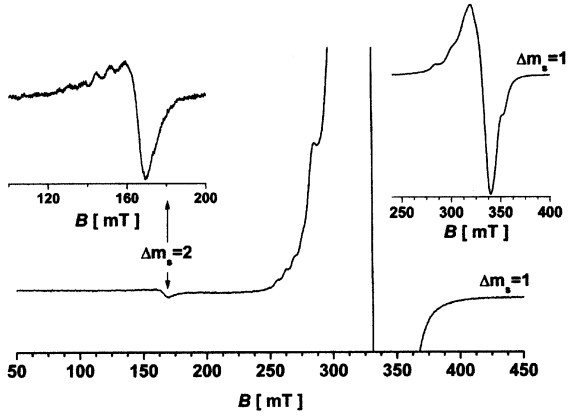

Figure 3. EPR spectra of $[Cu_3L]^{6+}$ (1.0 mM in MeCN/MeOH, 8:2). Instrumental parameters: frequency 9.664396 GHz, 100 kHz modulation frequency, 0.746 mT modulation amplitude, 80 μW microwave power, 168 s sweep time, 82 ms time constant, 6 scans, T = 4 K. The instrumental parameters for $\Delta m_s = 2$ transition were as follows: frequency 9.664377 GHz, 100 kHz modulation frequency, 0.746 mT modulation amplitude, 0.42 mW microwave power, 84 s sweep time, 82 ms time constant, 16 scans, T = 4 K.

This behaviour clearly indicates the presence of sizeable antiferromagnetic exchange terms (Js) active among the three Cu^{2+} metal ions and depopulation at lower temperature of higher spin states (S = 1 or S = 3/2). However, the one/third transition ($\Delta m_s = 3$) is not observed in the system. Furthermore, the intensity of the $\Delta m_s = 2$ transition is also rather weak, and thus, the axial ZFS component D needs to be small, as observed also for $[Cu_2L]^{4+}$. Drastic changes can be seen in the EPR spectrum of $[Cu_3L]^{6+}$ upon raising the temperature from cryogenic to T = 77 K, as shown in Figure 5B.

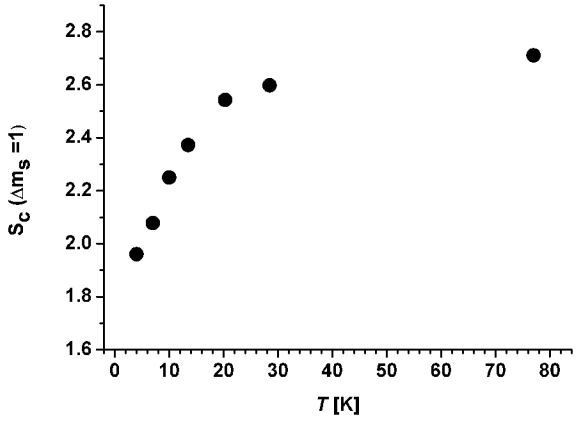

Figure 4. The variation of the spin concentration (S_c) of $[Cu_3L]^{6+}$ measured by following the double integrated $\Delta m_s = 1$ EPR line, normalized to CuEDTA standard, as a function of the temperature (T).

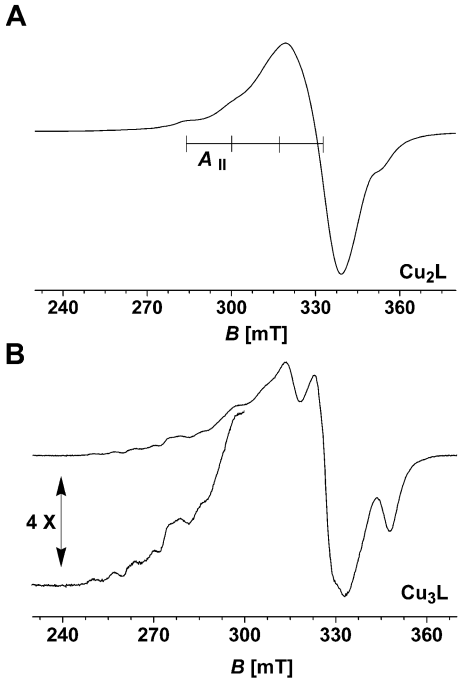

Figure 5. (A) EPR spectra of $[Cu_2L]^{4+}$ (1.3 mM in MeCN/MeOH, 8:2). Instrumental parameters: frequency 9.506573 GHz, 100 kHz modulation frequency, 0.5 mT modulation amplitude, 0.40 mW microwave power, 84 s sweep time, 82 ms time constant, 5 scans, T = 77 K. (B) EPR spectra of $[Cu_3L]^{6+}$ (1.0 mM in MeCN/MeOH, 8:2). Instrumental parameters: frequency 9.506582 GHz, 100 kHz modulation frequency, 0.5 mT modulation amplitude, 0.64 mW microwave power, 84 s sweep time, 82 ms time constant, 5 scans, T = 77 K.

Several weak resonances appear in the low-field region between g = 2.72 and g = 2.20 with at least two hyperfine terms for the three Cu^{2+} metal ions ($A_{\|1} = 6.7$ mT, $A_{\|2}$ = 13 mT) plus one well-defined resonance at high field at g = 1.95. No additional resonances are observed at much higher field (>400 mT) or lower field (<200 mT). The spin concentration accounts for $S_c = 2.70 \pm 0.11$ spins against CuEDTA standard, which is close to three uncorrelated

spins. Such a complicated EPR pattern and temperature behaviour observed for $[Cu_3L]^{6+}$ can be explained by using different spin models: (i) By the presence of a triplet species ($S = 1$) made by two weakly antiferromagnetically coupled Cu^{2+} ions overlapped with an isolated doublet species ($S = 1/2$, the third Cu^{2+}). (ii) By considering a three-spin system with population of the excited $S = 3/2$ state or $S = 1$ intermediate spin state in a three-spin frustrated system. (iii) With a three-spin system with very low symmetry; hence, not addressable as spin-frustrated. The hyperfine splitting pattern in spin-frustrated trigonal and distorted Cu_3 clusters (equilateral, isosceles and scalene triangles) was recently addressed in the literature.[20] In the case of scalene clusters, where all the J terms are different ($J_{1,2} \neq J_{2,3} \neq J_{1,3}$), the effective hyperfine constants and splitting strongly depend on the ratios (magnitude) of $J_{1,2}/J_{2,3}$ and $J_{1,2}/J_{1,3}$. However, the hyperfine splitting observed in $[Cu_3L]^{6+}$ does not seem to fulfill the requirements for a spin-frustrated Cu_3 system; most likely, it belongs to case (iii) and, hence, a very weakly dipolar coupled spin system. The results obtained through theoretical modelling the $[Cu_3L]^{6+}$ molecule (MM/UFF and metal–ligand coordination sphere refined by B3LYP/LanL2DZ) is shown in Figure 6B, and indicates that in the optimized structure the complex adopts a strained ligand conformation, with a small torsion angle between the naphthyl groups ($|\theta| = 75°$). This effect is clearly induced by coordination of the copper(II) ion to the nitrogen donors adjacent to the naphthyl rings (site B). The CuB–N4 (2.211 Å) and CuB–N5 (2.248 Å) distances are longer than those witnessed for the Cu–N (tertiary amino groups) at the A sites, with Cu1A–N3 of 2.143 Å and Cu2A–N8 of 2.168 Å. Furthermore, the metal to *N*-benzimidazole distances of the copper ions coordinated at the A sites are slightly elongated (Cu–N, 1.94 Å–1.96 Å) with respect to those observed in the dinuclear complex. The calculated intramolecular Cu1A–CuB–Cu2A distances of 5.7 Å (Cu1A–CuB), 5.9 Å (CuB–Cu2A) and 11.1 Å (Cu1A–Cu2A) agree with the earlier description of weakly dipolar coupled three spin-system.

In view of the absence of structural information, the molecular modelling results must be taken with caution. However, we speculate that the observed EPR spectrum recorded at 77 K arises from population of the quartet state and, hence, is an admixture of quartet and doublet states, where the $S = 1/2$ spin configuration represents the ground state. Furthermore, because of the lack of features at $g > 4$, a small axial term for the quartet state can be extracted ($|D| \approx 6 \times 10^{-3}\ cm^{-1}$) together with an overall exchange term(s) J among the copper centres very small ($<<4$ K) and negative.

Clear differences can be observed between $[Cu_2L]^{4+}$ and $[Cu_3L]^{6+}$ upon interaction with azido ligands, as shown in Figure 7.

Addition of two equivalents of azido ligand to $[Cu_2L]^{4+}$ (Figure 7A) leads to an adduct with two isolated Cu^{2+} ions under rather strong tetragonal field ($g_{\|} = 2.232$, $g_{\perp} = 2.059$ and $A_{\|} = 18.4$ mT). This is consistent with terminal coordination of the N_3^- molecules to the copper ions. In contrast, upon addition of two equivalents of azido to $[Cu_3L]^{6+}$, the resulting EPR spectrum measured at cryogenic temperature shows the fingerprints of populated high-spin states [Figure 7B, trace (a)] with several resonances ranging from $g = 10.5$ to $g = 1.47$ plus the signal of mononuclear Cu centre

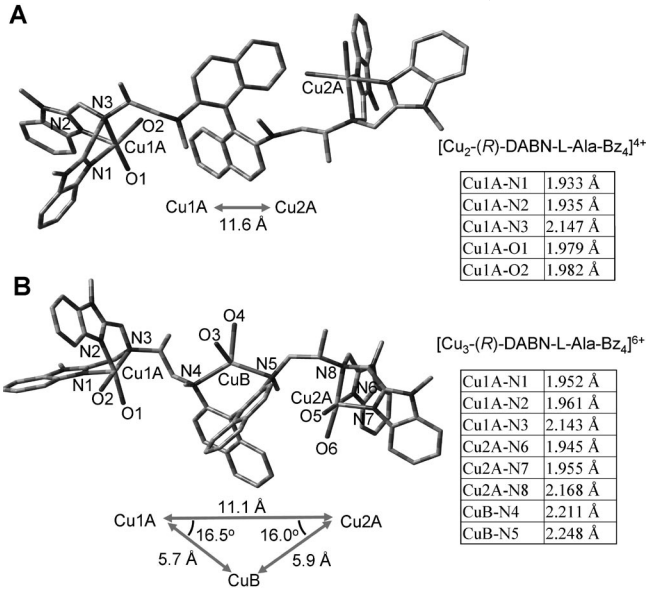

Figure 6. Capped sticks drawings of the optimized geometry (MM/UFF for the molecular backbone and DFT/B3LYP/LanL2DZ for the copper coordination spheres) for the dinuclear (A) and trinuclear (B) copper(II) complexes. Hydrogen atoms are not depicted for clarity.

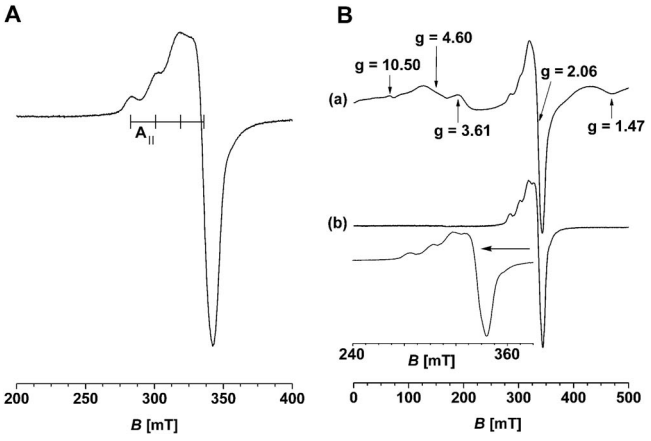

Figure 7. (A) EPR spectrum of $[Cu_2L]^{4+}$ (1.3 mM in MeCN/MeOH, 8:2) with 2 equiv. of N_3^-. Instrumental parameters: frequency 9.665649 GHz, 100 kHz modulation frequency, 0.746 mT modulation amplitude, 80 μW microwave power, 168 s sweep time, 82 ms time constant, 4 scans, $T = 4$ K. (B) Trace (a) EPR spectrum of $[Cu_3L]^{6+}$ (1.0 mM in MeCN/MeOH, 8:2) with 2 equiv. of N_3^-. Instrumental parameters: frequency 9.664006 GHz, 100 kHz modulation frequency, 0.746 mT modulation amplitude, 80 μW microwave power, 168 s sweep time, 82 ms time constant, 4 scans, $T = 4$ K. Trace (b) EPR spectrum of $[Cu_3L]^{6+}$ (1.0 mM in MeCN/MeOH, 8:2) with 3 equiv. of N_3^-. Instrumental parameters: frequency 9.664800 GHz, 100 kHz modulation frequency, 0.746 mT modulation amplitude, 80 μW microwave power, 168 s sweep time, 82 ms time constant, 4 scans, $T = 4$ K. The inset shows enlarged the relevant copper-signal region.

around g ≈ 2.1. This result indicates that both $S = 3/2$ and $S = 1/2$ ($g_{\parallel} = 2.230$, $g_{\perp} = 2.063$ and $A_{\parallel} = 17.5$ mT) are populated and, furthermore, a larger *ZFS* parameter ($|D| > 0.06$ cm^{-1}) characterizes the three spin system. In addition to that, both azido molecules should act as bridges (μ-1,3) among the Cu^{2+} centres leading to a folded configuration for the $[Cu_3L]^{6+}$ complex. Further addition of the azido ligand, up to 3 equiv. per equiv. of complex, destroys such bridged configuration, and in fact only the signal of isolated copper centres appears in the spectrum [Figure 7B, trace (b)] with spin-Hamiltonian parameters $g_{\parallel} = 2.225$, $g_{\perp} = 2.058$, $A_{\parallel} = 18.5$ mT. Furthermore, its EPR resonance line is characterized by loss of both high- and low-field components. This result suggests that N_3^- molecules bind as terminal ligands to the copper ions with loss of appreciable interaction among the copper centres. Here the metal coordination spheres of the azido adduct of $[Cu_3L]^{6+}$ need to be similar to those present in the azido adduct of $[Cu_2L]^{4+}$ (Figure 7A). This is due to the similarities witnessed in their overall EPR envelopes, spin-Hamiltonian parameters and especially in $A_{\parallel}$. The question that emerges from these results is that only two N_3^- molecules seem to directly interact with the trinuclear copper cluster, in harmony with the above-described azido binding experiments to $[Cu_3L]^{6+}$. It is unclear why the third azido molecule does not directly bind to the copper closer to the binaphthyl residues, but merely destabilizes the azido bridges, leaving the other two copper centres coordinated by benzimidazole groups, actively involved in Cu–N_3^- bonds. However, in this setting, the overlapped features of two different types of coordination environments for the metal ions should arise in the EPR envelope, which indeed are not observed, even upon further dilution of the solution in order to minimize intermolecular effects. A possible explanation for the lack of EPR feature of the copper located by the binaphthyl groups is that its fingerprint must be masked by the dominating and broad components of the copper–N_3^- adducts coordinated by benzimidazole moieties (vide infra). Attempts were also made to obtain resonance Raman spectra (rR) on both frozen and liquid solutions of the Cu^{II} complexes and their azido adducts to gain information on the copper environments and the azido binding modes, but they were unsuccessful due to the strong fluorescence of these molecules under different laser excitation wavelengths (410 and 532.3 nm).

Nevertheless, additional insight into the nature of the copper complexes was obtained by following the changes in their EPR spectra after reaction with catechol as substrate (Figure 8).

The reactions were carried out anaerobically in acetonitrile solution, which is known to stabilize the Cu^{I} oxidation state, and by employing the less-reactive pyrocatechol as substrate, which was added to a chilled solution (in ice) of the complexes, followed by fast cooling to 77 K. After addition of 2 equiv. of catechol to $[Cu_2L]^{4+}$, nearly no Cu^{II} EPR signal ($S_c < 0.1$ spins against CuEDTA) was detected, and also absent was any signal attributable to a radical (semiquinone) species (Figure 8, grey line). Furthermore,

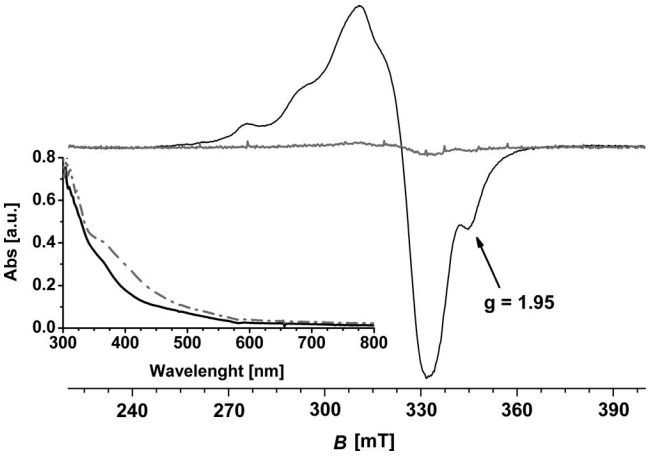

Figure 8. EPR spectra of $[Cu_2L]^{4+}$ (1.3 mM in MeCN/MeOH, 8:2; grey line) and $[Cu_3L]^{6+}$ (1.0 mM in MeCN/MeOH, 8:2; solid line) recorded immediately after addition of a small excess of pyrocatechol (2 equiv. per equiv. of complexes, MeCN/MeOH, 1:1). Instrumental parameters: frequency 9.435578 GHz ($[Cu_3L]^{6+}$) and 9.437768 GHz ($[Cu_2L]^{4+}$), 100 kHz modulation frequency, 0.5 mT modulation amplitude, 0.80 mW microwave power, 84 s sweep time, 82 ms time constant, 4 scans, $T = 77$ K. The inset shows the corresponding UV/Vis spectrum (1 mm quartz cuvette) of $[Cu_2L]^{4+}$ before (solid black line) and after (dashed-dotted grey line) addition of pyrocatechol.

the development of a band around 390 nm was observed in the UV/Vis spectrum after addition of the substrate (Figure 8 inset, dashed-dotted grey line), which is associated with the formation of the quinone species. Hence, the two copper ions of $[Cu_2L]^{4+}$ were reduced to Cu^{I} and the catechol was oxidized to quinone. A similar reaction occurred for $[Cu_3L]^{6+}$ upon addition of 2 equiv. of catechol, with development of the quinone band around 390 nm in the UV/Vis spectrum (data not shown). However, the dominant signal of a mononuclear Cu^{II} species remained clearly detectable in the EPR spectrum (Figure 8, black line) with spin-Hamiltonian parameters consistent with a Cu^{II} ion bound in a tetragonal environment ($g_{\parallel} = 2.239$, $g_{\perp} = 2.074$, $A_{\parallel} = 17.0$ mT) plus small additional resonances in the low-field region between g = 2.7–2.5, together with a more pronounced signal at g ≈ 1.95, all of which are reminiscent of the EPR fingerprints observed in the fully oxidized $[Cu_3L]^{6+}$ (see Figure 5B). The spin concentration accounted in this case for $S_c = 1.25 \pm 0.12$ spins against CuEDTA standard, which confirms the presence of a small fraction of fully oxidized $[Cu_3L]^{6+}$. Taking all these results into consideration and bearing in mind the EPR envelope of Cu^{II} observed for $[Cu_2L]^{4+}$, and those of $[Cu_3L]^{6+}$–azido adducts, the copper signal observed in Figure 8 for $[Cu_3L]^{6+}$ plus pyrocatechol mostly corresponds to the Cu^{II} ion bound to the two nitrogen atoms attached to the binaphthyl rings. Clearly, this metal centre does not participate in the binding and redox reaction with the substrate, although its presence is important in the chiral discrimination of substituted catechols. It is worth noting that in the parent trinuclear complexes derived from the (*R*)-DABN[7a] and (*S*)-DABN[7c] ligands, which are similar to L but contain simple

methylene carbon chains connecting CuB and the two CuA centres instead of the L-alanine residues, the coupled coppers were one CuA and CuB. Probably, this difference depends on the length of the carbon chain connecting the binaphthyldiamine nitrogen atoms of site B and the tertiary amine nitrogen atoms of the A sites, which is two carbon atoms long in L (Scheme 2) but three carbon atoms long in DABN.[7ac]

Stereoselective Catecholase Activity

To investigate the stereoselectivity in catalytic oxidations by the $[Cu_2L]^{4+}$ and $[Cu_3L]^{6+}$ complexes we chose a representative set of biogenic catechols[11] (L- and D-dopa, the corresponding methyl esters L- and D-dopaOMe and L- and D-norepinephrine) and two flavonoids[21] (D-catechin and L-epicatechin). The activity was evaluated by monitoring the growth of the absorption band due to the formation of quinone adducts with MBTH. As in the case of our previous studies with dinuclear and trinuclear Cu^{II} complexes,[7] a two-step mechanism of catechol oxidation can be hypothesized for the present biomimetic catalytic reactions. However, the kinetic experiments showed monophasic behaviour, and it was impossible to separate the two steps. For the $[Cu_2L]^{4+}$ complex, the dependence of the initial rates of the catalytic reactions on substrate concentration exhibited a hyperbolic behaviour, and the kinetic parameters were estimated by using the Michaelis–Menten equation. The $[Cu_3L]^{6+}$ complex behaved in the same way with substrates L-/D-dopa and L-/D-norepinephrine, whereas with L-/D-dopaOMe, D-catechin and L-epicatechin inhibition occurred at high substrate concentration, and therefore, the kinetic parameters had to be estimated by using the equation reported in our previous paper.[22] Some preliminary catalytic experiments carried out by using the mononuclear analogue $[CuL]^{2+}$ (prepared in situ) showed much lower reactivity with respect to the dinuclear and trinuclear counterparts (e.g., for the oxidation of L-dopaOMe the k_{cat}/K_M value was found to be 136 $M^{-1}s^{-1}$, at least one order of magnitude smaller than that of the parent complexes); therefore, the reactivity of the mononuclear complex was not considered further.

The dinuclear complex $[Cu_2L]^{4+}$ displays poor substrate enantiodifferentiating ability, as expressed by the R% index, in the oxidation of all catechols, even though it exhibits catalytic activity comparable to that of $[Cu_3L]^{6+}$ (Table 1), and also with the other Cu complexes derived from binaphthyl ligands.[7] As shown by EPR analysis and molecular modelling, in the dinuclear complex the nitrogen donors attached to the binaphthyl group do not coordinate to the Cu ions, and hence, the chiral residues, both from the binaphthyl group and the carbon chains containing L-alanine, are located rather apart from the redox metal centres. This makes the interaction between the chiral group of the substrates with those of the ligand extremely weak when catechols undergo reactions at the metal centres, resulting in little enantiodifferentiation in the catalytic reactions. In contrast, the trinuclear complex $[Cu_3L]^{6+}$ exhibits significant enantioselectivity in the oxidations of the catecholamines L-/D-dopaOMe and L-/D-norepinephrine. The origin of this enantioselectivity must be associated with the mode of substrate binding, as it depends almost entirely on K_M. It is interesting to note that the corresponding trinuclear complexes derived from the ligands (*R*)-DABN[7a] and (*S*)-DABN,[7c] which are topologically similar to L but containing the binaphthyl group as the only chiral element, exhibited almost negligible enantiodifferentiating power against L-/D-dopaOMe. In that case, however, catechol binding oc-

Table 1. Kinetic parameters for the stereoselective oxidation of the substrates in methanol/aqueous phosphate buffer, 50 mM, pH 8.6, in the presence of MBTH at 20 °C.

	$[Cu_2$-(*R*)-(+)-DABN-L-Ala-$Bz_4][ClO_4]_4$				
Substrate	K_M [M]	k_{cat} [s^{-1}]	k_{cat}/K_M [$M^{-1}s^{-1}$]	R%[a]	r^2[b]
L-dopa	$(1.89 \pm 0.25) \times 10^{-4}$	$(4.73 \pm 0.21) \times 10^{-3}$	25	11	0.98
D-dopa	$(2.58 \pm 0.35) \times 10^{-4}$	$(5.31 \pm 0.26) \times 10^{-3}$	20		0.98
L-dopaOMe	$(6.31 \pm 1.31) \times 10^{-6}$	$(9.43 \pm 0.45) \times 10^{-3}$	1493	6	0.96
D-dopaOMe	$(4.80 \pm 0.66) \times 10^{-6}$	$(6.41 \pm 0.45) \times 10^{-3}$	1335		0.93
L-norepinephrine	$(1.87 \pm 0.35) \times 10^{-5}$	$(5.12 \pm 0.16) \times 10^{-3}$	274	5	0.95
D-norepinephrine	$(2.05 \pm 0.34) \times 10^{-5}$	$(5.12 \pm 0.16) \times 10^{-3}$	250		0.95
D-catechin[c]	$(3.60 \pm 0.36) \times 10^{-5}$	$(2.77 \pm 0.11) \times 10^{-2}$	769	9	0.99
L-epicatechin[c]	$(4.81 \pm 0.37) \times 10^{-5}$	$(3.10 \pm 0.11) \times 10^{-2}$	644		0.99
	$[Cu_3$-(*R*)-(+)-DABN-L-Ala-$Bz_4][ClO_4]_6$				
Substrate	K_M [M]	k_{cat} [s^{-1}]	k_{cat}/K_M [$M^{-1}s^{-1}$]	R%[a]	r^2[b]
L-dopa	$(2.79 \pm 0.31) \times 10^{-4}$	$(9.35 \pm 0.40) \times 10^{-3}$	33	3	0.99
D-dopa	$(3.24 \pm 0.45) \times 10^{-4}$	$(1.01 \pm 0.06) \times 10^{-2}$	31		0.98
L-dopaOMe	$(3.89 \pm 0.44) \times 10^{-6}$	$(1.28 \pm 0.01) \times 10^{-2}$	3283	52	0.98
D-dopaOMe	$(1.01 \pm 0.11) \times 10^{-5}$	$(1.06 \pm 0.02) \times 10^{-2}$	1045		0.99
L-norepinephrine	$(5.06 \pm 0.55) \times 10^{-5}$	$(1.28 \pm 0.03) \times 10^{-2}$	254	27	0.98
D-norepinephrine	$(7.51 \pm 0.94) \times 10^{-5}$	$(1.10 \pm 0.03) \times 10^{-2}$	147		0.98
D-catechin[c]	$(5.05 \pm 0.48) \times 10^{-5}$	$(6.46 \pm 0.15) \times 10^{-2}$	1280	5	0.98
L-epicatechin[c]	$(5.08 \pm 0.37) \times 10^{-5}$	$(5.84 \pm 0.10) \times 10^{-2}$	1150		0.99

[a] $R\% = [(k_{cat}/K_M)_L - (k_{cat}/K_M)_d]/[(k_{cat}/K_M)_L + (k_{cat}/K_M)_D] \times 100$ is taken as the index of enantioselectivity in the catalytic reactions, except for D-catechin and L-epicatechin, where the L and D suffixes are inverted. [b] The coefficient of determination (r^2). [c] In methanol/aqueous phosphate buffer, 50 mM, pH 7.0, with MBTH at 20 °C.

curred to one CuA site and the CuB site, whereas here, according to the EPR experiments, the catechol binds to the two CuA sites. We have no evidence to assume that with $[Cu_3L]^{6+}$ the chiral amine portion of the catecholamines can interact directly with CuB, but clearly this portion is recognized by the complex only when this Cu centre is present. In particular, the discrimination is strong with L-/D-dopaOMe, where a bulky carboxymethyl substituent is present on the carbon atom in the 2-position from the catechol ring, whereas it decreases with the substrates carrying smaller hydroxy substituents (L-/D-norepinephrine and the flavonoids). Probably the presence of CuB imposes a folded conformation to the ligand L generating some steric interaction between the binaphthyl chromophore (and possibly also the L-Ala methyl group) with the substituent chain of the catechol, which becomes particularly strong with D-dopaOMe, as reflected by the large value of K_M.

Regarding the lack of recognition between L-/D-dopa by both $[Cu_2L]^{4+}$ and $[Cu_3L]^{6+}$, we note that this effect is common to all 1,1′-binaphthyl-derived dinuclear and trinuclear Cu complexes.[7ac] With L-/D-dopa as substrates, binding of the catechol residue to the Cu centres suffers strong competition by the polar amino acid portion, which is strongly chelating, and this is reflected by the comparatively much larger K_M values observed with these substrates (Table 1).[7ac] Thus, assuming that in the productive binding the catechol residue of L-/D-dopa binds to the CuA centres, this leaves the amino group and particularly the charged carboxylate group on the side chain either interacting with CuB, as in $[Cu_3L]^{6+}$, or with the free amine groups attached to, but displaced from the binaphthyl rings, as in $[Cu_2L]^{4+}$. In both cases, we expect that there will be little recognition of the substrate chirality by the binaphthyl chromophore.

Experimental Section

Materials and Physical Methods: Compounds and solvents accessible from commercial sources were of highest purity available and used as received. Acetonitrile (spectral grade) was distilled from potassium permanganate and from sodium carbonate; it was then stored over calcium hydride and distilled before use under an inert atmosphere (UV cutoff <190). Tetrahydrofuran was dried by refluxing and distilling from metallic sodium. Dimethylformamide (DMF) was purified by treatment with barium oxide and distilled from calcium hydride under reduced pressure. Anhydrous methanol was obtained with activated 3 Å molecular sieves. Phosphate buffer solutions were prepared with water purified in a Millipore MilliQ system. Elemental analyses were performed at the Microanalytical Laboratory of the Chemistry Department in Milan with a Perkin–Elmer 2400 Analyzer. Optical rotations were obtained with a Perkin–Elmer 241 polarimeter at 25 °C by using a quartz cell of 10 cm path length. Mass spectra (MS) were obtained by using a Thermo-Finnigan LCQ Advantage electrospray ionization (ESI) mass spectrometer. Atomic absorption measurements were performed with a Perkin–Elmer 3100 AAS spectrometer. ICP measurements were obtained by using a Thermo-Jarrel Ash IRIS INTREPID. UV/Vis spectra were recorded from HP 8452A or HP 8453 diode array spectrophotometers equipped with a magnetically stirred, thermostatted cell holder maintained at 20 ± 0.1 °C. Circular dichroism (CD) spectra were recorded with a Jasco J-500 spectropolarimeter by using quartz cells of 0.1–2.0 cm path length. ^1H and ^{13}C NMR spectra were recorded with a Bruker AVANCE 400 spectrometer operating at 9.37 T. The EPR measurements were performed with a dual-band X-cavity (quality factor Q = 3000–4000) or a standard X-band cavity (quality factor Q = 2200–3000) with a Bruker Elexsys 500E spectrophotometer equipped with a He-flow cryostat (ESR 900, Oxford Instruments) or by using a nitrogen bath-finger for the 77 K experiments. The solutions of both complexes and azido adducts were, prior to measurements, degassed by exchange with argon to avoid possible signals broadening at low temperature due to the presence of oxygen. All the EPR spectra were baseline corrected upon subtraction of the cavity background. CuEDTA standard solution (1 mM MeOH/CH_3CN, 8:2) was used for the spin concentration measurements.

The geometry optimization of the dinuclear and trinuclear copper complexes was performed through the molecular mechanics (UFF) force field method,[23] with guess method Extended Huckel, as implemented in the Gaussian 03 software (Gaussian 03W, v.6.0).[24] Some constraints were applied within optimization to the aromatic cores (intraring torsions for benzimidazole and naphthyl moieties). The geometries around the metal ions were further fully optimized by density functional methods (UHF/DFT). Beckes three-parameter hybrid-exchange functional and the correlation functionals from Lee, Yang and Parr (B3LYP) with LanL2DZ basis set were used for the copper ions, and the nitrogen and oxygen donors (Cu-coordination sphere), whereas the 6-31G* basis set was used for the next adjacent main group elements. The coordination spheres of the coppers were arbitrarily filled with coordinated hydroxide groups. The geometry optimization of the ligand (*R*)-(+)-DABN-L-Ala-Bz_4 was performed by using the PM3MM method, also implemented in Gaussian 03.[24] All calculations were performed by using the TITAN computer facilities at the University of Oslo. The Gaussian View (4.1.2) program was used for the molecular drawings.

(*R*)-(+)-DABN-L-Ala-Bz_4 (L): Prepared by following the synthetic route reported in Scheme 1.

2: Commercial (*R*)-(+)-DABN (1.61 g, 5.66 mmol) was dissolved in anhydrous chloroform (60 mL) under an atmosphere of nitrogen and cooled to 0 °C. A solution of *Z*-L-Ala-OH [*Z* = *N*-(benzyloxy)-carbonyl; 2.53 g, 11.33 mmol], 1-hydroxybenzotriazole (HOBT; 1.84 g, 13.58 mmol), *N*-(3-dimethylaminopropyl)-*N*′-ethylcarbodiimide hydrochloride (EDC·HCl; 2.60 g, 13.58 mmol) in anhydrous chloroform (100 mL) under an atmosphere of nitrogen and cooled to 0 °C was then added dropwise to the above solution over 15–20 min. The mixture was subsequently warmed to room temperature and stirred for 2 d. The reaction, monitored by TLC (silica gel; toluene/*tert*-butyl methyl ether, 6:4), was then quenched by the addition of 1 N HCl (150 mL). The organic layer was separated and treated with a saturated solution of sodium hydrogen carbonate (2 × 150 mL) and finally with brine (150 mL). Then, the chloroform solution was dried with Na_2SO_4 and filtered, and the solvent was removed by rotary evaporation to give a brown, oily product (3.43 g). The crude product was purified by silica flash chromatography (3 × 20 cm) under the following conditions: pressure, 1 inch min^{-1}; eluent, toluene/*tert*-butyl methyl ether, 90:10 to 50:50 (each fraction 100 mL). The first eluted fraction consisted of the unreacted diamine, followed by desired product **2** and finally by the monocondensed compound. To increase the yield, the monocondensed product was treated again with stoichiometric amounts of *Z*-L-Ala-OH, HOBT and EDC·HCl in chloroform solution, under the same conditions as reported above to give a further amount of compound **2**. The total yield of the white powder was 65%.

$[\alpha]_D^{20}$ = +12.44 (c = 1.61 × 10^{-2} M, $CHCl_3$). MS (ESI): m/z (%) = 694 (100) [M + 1]. ^{1}H NMR (400 MHz, $CDCl_3$, 25 °C): δ = 1.22 (d, ^3J = 5.7 Hz, 6 H, CH_3-CH), 4.19 (m, 2 H, CH-CH_3), 4.60–4.88 (m, ^2J = 12.3 Hz, 4 H, CH_2-C_6H_5), 5.38 (d, ^3J = 5.1 Hz, 2 H, H-N-CH), 7.11–7.82 (m, ^3J = 7.5 Hz, ^3J = 7.5 Hz, ^3J = 8.4 Hz, 8 H, CH-binaphthyl), 7.30–7.40 (m, 10 H, CH-C_6H_5), 7.75 (s, 2 H, H-N-binaphthyl), 7.85–8.17 (d, ^3J = 8.4 Hz, 4 H, CH-binaphthyl) ppm. ^{13}C NMR (100.6 MHz, $CDCl_3$, 25 °C): δ = 16.9, 50.8, 66.9, 122.9, 123.2, 125.5, 125.9, 127.3, 127.8, 128.1, 128.2, 128.5, 129.8, 131.5, 132.4, 133.9, 136.1, 156.1, 171.6 ppm. UV/Vis (CH_3CN): λ (ε, M^{-1} cm^{-1}) = 216 (31800), 245 (79300), 255 (sh.; 37500), 285 (15800), 300 (sh.; 12900), 336 (3700), 353 (sh.; 2100) nm. CD (CH_3CN): λ ($\Delta\varepsilon$, M^{-1} cm^{-1}) = 204 (+96.4), 217 (–56.4), 230 (+18.6), 247 (–88.7), 261 (sh.; –11.8), 284 (+26.4), 318 (+2.8) nm. $C_{42}H_{38}N_4O_6$ (694.77): calcd. C 72.61, H 5.51, N 8.06; found C 72.44, H 5.68, N 8.00.

3: To a solution of compound **2** (0.14 g, 0.202 mmol) dissolved in anhydrous methanol (10 mL) was added palladium–charcoal (10% palladium content, 50 mg), and the mixture was hydrogenated at atmospheric pressure with stirring until carbon dioxide evolution ceased. The catalyst was removed by filtration through Celite, and the filtrate was evaporated to dryness under vacuum. The oily residue was triturated with diethyl ether and filtered to obtain a white compound that was dried under vacuum. Yield 96%. $[\alpha]_D^{20}$ = +57.38 (c = 2.09 × 10^{-2} M, CH_3OH). MS (ESI): m/z (%) = 427 (100) [M + 1]. ^{1}H NMR (400 MHz, CD_3OD, 25 °C): δ = 0.86 (d, ^3J = 6.9 Hz, 6 H, CH_3-CH), 3.19 (m, 2 H, CH-CH_3), 7.09–7.97 (m, ^3J = 8.4 Hz, ^3J = 8.1 Hz, ^3J = 8.1 Hz, ^4J = 1.2 Hz, ^4J = 1.2 Hz, 8 H, CH-binaphthyl), 8.07–8.13 (m, ^3J = 8.9 Hz, 4 H, CH-binaphthyl) ppm. ^{13}C NMR (100.6 MHz, $CDCl_3$, 25 °C, TMS): δ = 124.2, 126.0, 126.4, 126.8, 128.1, 129.4, 130.4, 133.3, 134.1, 135.7, 177.4 ppm. UV/Vis (CH_3CN): λ (ε, M^{-1} cm^{-1}) = 220 (sh.; 35800), 245 (74000), 255 (sh.; 61000), 288 (15300), 300 (sh.; 12600), 322 (sh.; 4050), 336 (3800) nm. CD (CH_3CN): λ (ε, M^{-1} cm^{-1}) = 203 (+94.7), 216 (–48.0), 230 (+19.4), 247 (–88.5), 259 (sh.; –8.6), 284 (+31.6), 296 (sh.; +14.9), 335 (–2.3) nm. $C_{26}H_{26}N_4O_2$ (426.51): calcd. C 73.22, H 6.14, N 13.14; found C 73.45, H 6.24, N 13.06.

4: To a solution of compound **3** (0.369 g, 0.864 mmol) dissolved in dry DMF (10 mL) was added solid 2-chloromethyl-1-methylbenzimidazole (0.65 g, 3.63 mmol)[10b] and dry sodium carbonate (0.55 g, 5.185 mmol), and the stirred mixture was warmed to 80 °C for 6 h under an atmosphere of nitrogen. The reaction was followed by TLC (silica gel; AcOEt/iPrOH/NH_3, 5:4:0.1). Unfortunately the product always showed the presence of mixtures of di-, tri- and tetracondensed fractions, even after the addition of excess reactant and by increasing the reaction time to 1 d. In this case, silica flash chromatography (2 × 20 cm) was performed to separate the single fractions under the following conditions: pressure 1 inch min^{-1}; eluent, AcOEt/iPrOH (5:4) and increasing amount of concentrated NH_3 (0 to 1%). The dicondensed product was obtained in pure form, whereas it was not possible to separate the other fractions. These fractions were allowed to react, after drying, under the following conditions: the mixture of tri- and tetracondensed products (0.53 g) was dissolved in dry DMF (20 mL) and 2-(chloromethyl)-1-methylbenzimidazole (0.48 g, 2.66 mmol) and dry sodium carbonate (0.35 g, 3.28 mmol) were then added, and the stirred mixture was warmed to 80 °C for 2 d under an atmosphere of nitrogen. The TLC (silica gel) of the mixture showed that only a minimum amount of tricondensed product was present and then, after cooling, the precipitate so obtained was filtered off. It consisted of a mixture of products and inorganic salts and was thus treated with chloroform and filtered again. The combined filtrates were dried under vacuum to afford a brown oily that was purified by silica flash chromatography (AcOEt/iPrOH, 5:4) and an increasing amount of concentrated NH_3 (0 to 1%) (each fraction 180 mL). A light-orange solid was obtained in 42% yield. $[\alpha]_D^{20}$ = –30.50 (c = 1.79 × 10^{-3} M, $CHCl_3$). MS (ESI): m/z (%) = 1003 (100) [M + 1]. ^{1}H NMR (400 MHz, $CDCl_3$, 25 °C): δ = 0.99 (d, ^3J = 7.2 Hz, 6 H, CH_3-CH), 3.39 (m, 2 H, CH-CH_3), 3.47 (s, 12 H, CH_3-N-benzimidazole), 3.50–3.69 (m, 8 H, CH_2-benzimidazole), 5.50 (s, 1 H, H-N-binaphthyl), 5.72 (s, 1 H, H-N-binaphthyl), 6.83–7.53 (m, ^3J = 8.4 Hz, ^3J = 8.4 Hz, ^3J = 5.6 Hz, 8 H, CH-binaphthyl), 7.04–7.53 (m, 16 H, CH-C_6H_4), 7.63–7.65 (m, ^3J = 4.8 Hz, 4 H, CH-binaphthyl) ppm. ^{13}C NMR (100.6 MHz, $CDCl_3$, 25 °C): δ = 10.2, 29.6, 47.1, 59.6, 108.9, 119.2, 121.7, 122.4, 124.8, 125.2, 125.9, 127.6, 128.3, 128.7, 131.5, 132.3, 134.5, 135.8, 141.7, 150.9, 172.6 ppm. UV/Vis (CH_3CN): λ (ε, M^{-1} cm^{-1}) = 207 (109500), 246 (33700), 256 (sh.; 28500), 278 (21700), 286 (20500), 302 (sh.; 11700), 335 (sh.; 4700), 370 (sh.; 3300) nm. CD (CH_3CN): λ (ε, M^{-1} cm^{-1}) = 208 (+31.1), 219 (–44.3), 247 (–16.6), 255 (–15.5), 263 (sh.; –6.7), 281 (+6.7), 290 (sh.; +5.2) nm. $C_{62}H_{58}N_{12}O_2$ (1003.2): calcd. C 74.23, H 5.83, N 16.75; found C 73.95, H 5.94, N 16.86.

5: Compound **5** was prepared in accordance to the procedure outlined by Marino et al.,[25] with slight modifications: Compound **4** (0.22 g, 0.209 mmol) was stirred with NaH (0.158 g, 6.58 mmol, washed three times with n-pentane) in dry DMF (10 mL) for 20 min at 20 °C. After cooling the mixture to 0 °C, CH_3I (0.934 g, 6.58 mmol, 409.5 μL) diluted in dry DMF (1 mL) was added dropwise over 10 min, and stirring was continued for a further 2 h at room temperature. The mixture was then poured into brine (25 mL) and the N-methylated compound was extracted with CH_2Cl_2 (3 × 30 mL). The CH_2Cl_2 extract was washed with brine (4 × 90 mL), the organic layer was dried with $MgSO_4$ and the solvent was removed by rotary evaporation. After drying under vacuum a brown oil was obtained that was treated with diethyl ether. The solvent was filtered off to furnish a slightly pink powder in 87% yield. $[\alpha]_D^{20}$ = –36.54 (c = 2.33 × 10^{-3} M, $CHCl_3$). MS (ESI): m/z (%) = 1031 (100) [M + 1]. ^{1}H NMR (400 MHz, $CDCl_3$, 25 °C): δ = 0.92 (d, ^3J = 7.2 Hz, 6 H, CH_3-CH), 2.87 (s, 6 H, CH_3-N-binaphthyl), 3.39 (m, 2 H, CH-CH_3), 3.47 (s, 12 H, CH_3-N-benzimidazole), 3.50–3.69 (m, 8 H, CH_2-benzimidazole), 6.61–7.67 (m, ^3J = 8.4 Hz, ^3J = 8.4 Hz, ^3J = 5.6 Hz, 8 H, CH-binaphthyl), 7.04–7.53 (m, 16 H, CH-C_6H_4), 7.82–8.03 (m, ^3J = 4.8 Hz, 4 H, CH-binaphthyl) ppm. ^{13}C NMR (100.6 MHz, $CDCl_3$, 25 °C): δ = 15.2, 29.5, 31.4, 46.7, 59.6, 109.5, 119.4, 120.5, 122.0, 124.8, 126.0, 126.7, 127.6, 128.0, 128.5, 129.6, 132.3, 134.5, 136.0, 142.1, 152.0, 172.6 ppm. UV/Vis (CH_3CN): λ (ε, M^{-1} cm^{-1}) = 205 (119500), 246 (37900), 258 (sh.; 28400), 278 (24000), 286 (23300), 302 (sh.; 10500), 346 (sh.; 5200), 393 (sh.; 3600) nm. CD (CH_3CN): λ (ε, M^{-1} cm^{-1}) = 212 (+25.4), 226 (sh.; –18.2), 232 (–20.5), 239 (sh.; –16.9), 247 (sh.; –14.8), 258 (sh.; –9.1), 283 (+6.9), 297 (sh.; +2.4) nm. $C_{64}H_{62}N_{12}O_2$ (1031.26): calcd. C 74.54, H 6.06, N 16.30; found C 74.45, H 6.24, N 16.06.

6: A solution of BH_3·Me_2S (1.04 g, 13.7 mmol, 1.3 mL) in dry THF (10mL) was added dropwise to a suspension of **5** (0.24 g, 0.229 mmol) in dry THF (20 mL) at 0 °C under an atmosphere of nitrogen. The temperature was then raised, and the solvent and Me_2S were slowly distilled off over 5 h while fresh, dry THF (100 mL) was added. The solvent was removed under vacuum, and a solution of MeOH/6 N HCl (4:1, 30 mL) was added dropwise at 0 °C to the solid residue. The mixture was then heated at reflux for 2 h. After cooling, the solution was evaporated, and the residue, cooled with ice bath, was treated with a 15% solution of Na_2CO_3 (50 mL) until basic pH. The aqueous solution, saturated with NaCl, was extracted with CH_2Cl_2 (5 × 60 mL). The organic layer was dried with $MgSO_4$, and the solvent was removed by rotary

evaporation under vacuum. The crude compound was purified by silica flash chromatography (2 × 20 cm) under the following conditions: pressure, 1 inch min^{-1}; eluent, CH_2Cl_2/MeOH, 10:0 to 0:10 (each fraction 25 mL). The fractions containing the pure compound were evaporated to yield a dark brown powder in 47% yield. $[\alpha]_D^{20}$ = –51.05 (c = 1.99 × 10^{-3} M, $CHCl_3$). MS (ESI): m/z (%) = 1003 (100) [M + 1]. ^{1}H NMR (400 MHz, $CDCl_3$, 25 °C): δ = 0.88 (d, ^3J = 7.2 Hz, 6 H, CH_3-CH), 2.82 (m, 2 H, CH-CH_3), 3.24 (s, 6 H, CH_3-N-binaphthyl), 3.22–3.33 (m, 8 H, CH_2-benzimidazole), 3.64–3.67 (^2J = 14.4 Hz, 8 H, CH_2-N-binaphthyl), 3.72 (s, 12 H, CH_3-N-benzimidazole), 6.54–7.09 (m, ^3J = 6.4 Hz, ^3J = 7.6 Hz, ^3J = 7.6 Hz, 8 H, CH-binaphthyl), 7.09–7.73 (m, 16 H, CH-C_6H_4), 7.54–7.93 (m, ^3J = 8.8 Hz, 4 H, CH-binaphthyl) ppm. ^{13}C NMR (100.6 MHz, $CDCl_3$, 25 °C): δ = 9.2, 13.7, 29.3, 29.6, 45.9, 52.3, 62.2, 108.9, 109.0, 109.2, 118.9, 119.3, 120.0, 121.8, 122.0, 122.2, 122.4, 122.8, 126.0, 128.1, 128.5, 128.8, 129.7, 130.9, 134.1, 135.7, 135.8, 141.9, 142.2, 151.4, 153.7 ppm. UV/Vis (CH_3CN): λ (ε, M^{-1} cm^{-1}) = 208 (61100), 255 (24000), 271 (sh.; 23500), 278 (12300), 285 (11100), 306 (sh.; 5300), 361(2470) nm. CD (CH_3CN): λ (ε, M^{-1} cm^{-1}) = 211 (+42.0), 225 (–29.5), 242 (–3.0), 257 (–21.2), 293 (+4.8), 370 (–1.4) nm. $C_{64}H_{66}N_{12}$ (1003.29): calcd. C 76.62, H 6.63, N 16.75; found C 76.45, H 6.74, N 16.56.

Unambiguous assignment of the ^{1}H NMR and ^{13}C NMR signals was obtained from the combination of ^{1}H–^{13}C HMQC, ^{1}H–^{1}H COSY and DEPT 135 spectra for all the intermediate compounds.

[Cu_2-(*R*)-DABN-L-Ala-Bz_4][ClO_4]$_4$·2H_2O: To a solution of (*R*)-DABN-L-Ala-Bz_4 (0.042 g, 0.042 mmol) in MeCN (5 mL) was added copper perchlorate hexahydrate (0.0292 g, 0.0788 mmol) dissolved in MeOH (2 mL). The resulting red-wine solution was stirred at room temperature for 2 h and then evaporated to a small volume (2 mL) and treated with diethyl ether (5 mL). The red-wine product was filtered, washed with water (≈1 mL) and dried under vacuum. Yield 87%. UV/Vis (CH_3CN): λ (ε, M^{-1} cm^{-1}) = 208 (89800), 228 (sh.; 43300), 248 (sh.; 25500), 272 (20300), 280 (19500), 300 (8200), 394 (sh.; 2410), 487 (sh.; 1500), 515 (1570) nm. CD (CH_3CN): λ (ε, M^{-1} cm^{-1}) = 214 (+13.51), 225 (sh.; –1.33), 234 (–3.32), 255 (–7.35), 291 (+3.86), 325 (–0.28), 403 (–0.09), 522 (+0.05) nm. $C_{64}H_{66}Cl_4Cu_2N_{12}O_{16}$·2$H_2O$ (1564.21): calcd. C 49.14, H 4.51, Cu 8.12, N 10.75; found C 49.54, H 4.65, Cu 8.14, N 10.61.

[Cu_3-(*R*)-DABN-L-Ala-Bz_4][ClO_4]$_6$·3H_2O: To a solution of (*R*)-DABN-L-Ala-Bz_4 (0.039 g, 0.039 mmol) in MeCN (10 mL) was added copper perchlorate hexahydrate (0.047 g, 0.127 mmol) dissolved in MeOH (2 mL). The resulting brown solution was stirred at reflux for 2 d and after cooling the mixture was evaporated to a small volume (2 mL) and treated with diethyl ether (5 mL). The violet product was filtered, washed with water (2 × ≈1 mL) and dried under vacuum. Yield 77%. UV/Vis (CH_3CN): λ (ε, M^{-1} cm^{-1}) = 206 (101900), 228 (52900), 272 (28300), 280 (26500), 302 (sh.; 12900), 366 (sh.; 5770), 380 (sh.; 5200), 497 (sh.; 2800), 529 (sh.; 2250), 630 (sh.; 820) nm. CD (CH_3CN): λ (ε, M^{-1} cm^{-1}) = 217 (+7.77), 235 (sh.; –1.34), 256 (–2.28), 291 (+1.98), 346 (–0.23), 406 (–0.15), 481 (–0.04), 630 (–0.04) nm. $C_{64}H_{66}Cl_6Cu_3N_{12}O_{24}$·3$H_2O$ (1844.68): calcd. C 41.67, H 3.93, N 9.11, Cu 10.33; found C 41.48, H 4.00, N 9.01,Cu 10.39.

Caution! Perchlorate complexes with organic ligands are potentially explosive and should be handled with great care. Only small amounts of material should be prepared. We did not have problems working with small amounts of the perchlorate complexes described in this paper.

Determination of Molar Absorptivities of the Quinones: It is well known that dinuclear and trinuclear model complexes, like tyrosinase, oxidize *o*-diphenols, triphenols and flavonoids to quinones, but, in all cases, the resulting quinones undergo further noncatalytic polymerization to produce melanic compounds. To prevent further reactions of the quinones initially formed, a nucleophilic reagent, 3-methyl-2-benzothiazolinone hydrazone (MBTH), that traps the quinones and generates chromophoric adducts, was used. Unfortunately, no molar absorptivities of these adducts for all the substrates were available, so a spectrophotometric method to determine the λ_{max} and the molar absorptivities of the adducts was performed. In general, the method is based on the oxidation of the substrates with an excess amount of sodium periodate, conditions under which the reaction was very fast.[26] The unstable quinones were trapped by the nucleophilic MBTH, and the λ_{max} was detected. In all the experiments only one band developed in the range 300–900 nm, which corresponds to the quinone adducts with MBTH. At the recorded λ_{max}, a series of experiments carried out with different substrate concentrations allowed the molar absorptivities of the different quinones to be determined by fitting the data to the Lambert–Beer equation. For D-catechin (+CQ), the experimental conditions were: λ_{max} = 459 nm; 50 mM phosphate buffer (pH 7.0)/MeOH (9:1) at 20.0 ± 0.1 °C; 2 mM $NaIO_4$; 1 mM MBTH; [+CQ] from 5 μM to 40 μM; quartz cell 1 cm path length; final volume in the cell 2 mL. The coefficient of determination (r^2) was 0.998 and the molar absorptivity was 17230 M^{-1} cm^{-1}. For L-epicatechin (-EQ) the experimental conditions were: λ_{max} = 463 nm; 50 mM phosphate buffer (pH 7.0)/MeOH (9:1) at 20.0 ± 0.1 °C; 2 mM $NaIO_4$; 1 mM MBTH; [-EQ] from 5 μM to 45 μM; quartz cell 1 cm path length; final volume in cell 2 mL. The coefficient of determination (r^2) was 0.994 and the molar absorptivity was 18950 M^{-1} cm^{-1}. For L-norepinephrine L-bitartrate the experimental conditions were: λ_{max} = 511 nm; 50 mM phosphate buffer (pH 8.6)/MeOH (9:1) at 20.0 ± 0.1 °C; 2 mM $NaIO_4$; 1 mM MBTH; substrate concentrations from 10 μM to 100 μM; quartz cell 1 cm path length; final volume in cell 2 mL. The coefficient of determination (r^2) was 0.992 and the molar absorptivity was 4835 M^{-1} cm^{-1}. A similar value was obtained for D-norepinephrine L-bitartrate.

Catalytic Oxidations of *o*-Diphenols and Flavonoids: The kinetics of catalytic oxidation of the *o*-diphenols L-dopa, D-dopa, L-dopaOMe, D-dopaOMe, L-norepinephrine and D-norepinephrine were studied by UV/Vis spectroscopy by using a magnetically stirred and thermostatted 1-cm path length cell. The temperature during the measurements was kept constant at 20 ± 0.1 °C. A mixture of aqueous phosphate buffer (50 mM, pH 8.6)/methanol (9:1) saturated with atmospheric oxygen was used as solvent. The experiments carried out over a substrate concentration range were initiated by adding a few microlitres of solutions of the complexes (final concentrations 2.65 × 10^{-6} M) in all the experiments, whereas the substrate concentration was varied from 4.0 × 10^{-6} to 8.1 × 10^{-4} M (final volume 2 mL). As reported above, to prevent further reactions of the quinones initially formed, an excess amount of MBTH (1.0 × 10^{-3} M) was added. The formation of the corresponding stable *o*-quinones-MBTH adducts was followed through the development of the strong absorption band at 500 nm for L-/D-dopa and their methyl ester (ε_{500} = 13400 M^{-1} cm^{-1} for dopa-*o*-quinone-MBTH, ε_{500} = 11600 M^{-1} cm^{-1} for dopaOMe-*o*-quinone-MBTH) and at 511 nm for L-/D-norepinephrine (ε_{511} = 4835 M^{-1} cm^{-1} for norepinephrine-*o*-quinone-MBTH).

The catalytic oxidations of the flavonoids L-epicatechin and D-catechin were studied by UV/Vis spectroscopy by using a mixture of aqueous phosphate buffer (50 mM, pH 7.0)/methanol (9:1) saturated with atmospheric oxygen as solvent. The experiments were carried out as reported above for the other substrates and, also in this case, MBTH (1.0 × 10^{-3} M) was added to prevent further reactions of the quinones initially formed. The formation of the stable

quinone–MBTH adducts was followed through the development of the strong absorption band at 463 nm (ε_{463} = 18950 $M^{-1}cm^{-1}$) for L-epicatechin–quinone–MBTH and at 459 nm (ε_{459} = 17230 $M^{-1}cm^{-1}$) for D-catechin–quinone–MBTH. In all the experiments, the noise was reduced by reading the absorbance difference between the λ_{max} of the adducts and that at 900 nm, and the initial rates of oxidation were obtained by fitting the absorbance versus time curves in the first few seconds of the reactions.

Ligand Binding Studies: Spectrophotometric titrations for the binding of azido ligands to $[Cu_2$-(*R*)-DABN-L-Ala-$Bz_4]^{4+}$ and $[Cu_3$-(*R*)-DABN-L-Ala-$Bz_4]^{6+}$ were carried out by adding concentrated methanol solutions of the ligand to solutions of the complexes dissolved in acetonitrile. Titration of $[Cu_2$-(*R*)-DABN-L-Ala-$Bz_4]^{4+}$ (1.325×10^{-4} M) was performed by addition of subsequent and equal amounts of an azido solution (9.63×10^{-2} M) from 0.2 to 2.0 [azido]/[Cu_2] ratios (each aliquot corresponding to a 0.2 ratio) and from 2.0 to 10.0 [azido]/[Cu_2] ratios (each aliquot corresponding to a 0.5 ratio). Further addition of azido to the dinuclear compound did not produce any changes in the LMCT band. In all cases it was found that binding of the anion is slow, so that incubation of the solutions was necessary (3 min after adding each aliquot) before the spectroscopic measurements, and it was impossible to separate the titration steps at various [N_3^-]/[Cu_2] ratios. In a similar way, titration of $[Cu_3$-(*R*)-DABN-L-Ala-$Bz_4]^{6+}$ (7.785×10^{-5} M) was carried out by addition of subsequent and equal amounts of azido (9.63×10^{-2} M) from 0.2 to 2.0 [azido]/[Cu_3] ratios (each aliquot corresponding to a 0.2 ratio), and from 2.0 to 5.0 [azido]/[Cu_3] ratios (each aliquot corresponding to a 0.5 ratio). In this case, further addition of azido up to three equivalents per equivalent of the trinuclear complex produced precipitation of the complex. Incubation of the mixtures was necessary, and it was impossible to separate the binding process into steps.

Acknowledgments

This work was supported by the Italian MIUR through a FIRST project. K. K. A. thanks the Norwegian Research Council for Grant 177661/V30. L. C. thanks the University of Pavia for a FAR grant.

[1] a) H. Beinert, *J. Biol. Chem.* **2002**, *277*, 37967–37972; b) R. N. Mukherjee, *Indian J. Chem.* **2003**, *42A*, 2175–2184; c) G. Parkin, *Chem. Rev.* **2004**, *104*, 699–767; d) H. J. Himmel, A. Schultz, G. Knoer, N. Lehnert, *Nachr. Chem.* **2006**, *54*, 214–233; e) D. M. Taylor, D. R. Williams, *Introduction to the Principles of Drug Design and Action*, 4th ed., CRC Press LLC, Boca Raton, Florida, **2006**, pp. 617–642.

[2] a) D. S. Tawfik, Z. Eshhar, B. S. Green, *Mol. Biotechnol.* **1994**, *1*, 87–103; b) M. D. Distefano, H. Kuang, D. Qi, A. Mazhary, *Curr. Op. Struct. Biol.* **1998**, *8*, 459–465; c) H.-H. Liu, Y.-Q. Wan, G.-L. Zou, *J. Electroan. Chem.* **2006**, *594*, 111–117; d) Y. Wei, M. H. Hecht, *Prot. Engin. Des. Sel.* **2004**, *17*, 67–75.

[3] a) L. Que Jr., W. B. Tolman, *Nature* **2008**, *455*, 333–340; b) J. Suh, W. S. Chei, *Curr. Opin. Chem. Biol.* **2008**, *12*, 207–213; c) A. Gavrilova, B. Bosnich, *Chem. Rev.* **2004**, *104*, 349–383; d) J. P. Collman, R. Boulatov, C. J. Sunderland, L. Fu, *Chem. Rev.* **2004**, *104*, 561–588; e) G. Battaini, A. Granata, E. Monzani, M. Gullotti, L. Casella, *Adv. Inorg. Chem.* **2006**, *58*, 185–233; f) E. Y. Tshuva, S. J. Lippard, *Chem. Rev.* **2004**, *104*, 987–1012.

[4] a) R. Noyori, *Asymmetric Catalysis in Organic Synthesis*, John Wiley & Sons, New York, **1994**; b) I. Ojima, *Catalytic Asymmetric Synthesis*, 2nd ed., Wiley-VCH, New York, **2000**; c) J. S. Seo, D. Whang, H. Lee, S. I. Jun, J. Oh, Y. J. Jeon, K. Kim, *Nature* **2000**, *404*, 982–986; d) R. M. Hazen, D. S. Sholl, *Nat. Mater.* **2003**, *2*, 367–374; e) T. Verbiest, S. V. Elshocht, M. Kauranen, L. Hellemans, J. Snauweart, C. Nuckolls, T. J. Katz, A. Persoons, *Science* **1998**, *282*, 913–915; f) I. Agranat, H. Caner, J. Caldwell, *Nat. Rev. Drug Discovery* **2002**, *1*, 753–768; g) C. Dhenaut, I. Ledoux, I. D. W. Samuel, J. Zyss, M. Bourgault, H. Le Bozec, *Nature* **1995**, *374*, 339–342; h) A. Prasanna de Silva, *Nature* **1995**, *374*, 310–311.

[5] a) L. Santagostini, M. Gullotti, R. Pagliarin, E. Bianchi, L. Casella, E. Monzani, *Tetrahedron: Asymmetry* **1999**, *10*, 281–295; b) L. Santagostini, M. Gullotti, R. Pagliarin, E. Monzani, L. Casella, *Chem. Commun.* **2003**, 2186–2187.

[6] M. Gullotti, L. Santagostini, R. Pagliarin, S. Palavicini, L. Casella, E. Monzani, G. Zoppellaro, *Eur. J. Inorg. Chem.* **2008**, 2081–2089.

[7] a) M. C. Mimmi, M. Gullotti, L. Santagostini, A. Saladino, L. Casella, E. Monzani, R. Pagliarin, J. Mol. Catal. A **2003**, *204–205*, 381–389; b) M. C. Mimmi, M. Gullotti, L. Santagostini, R. Pagliarin, L. De Gioia, E. Monzani, L. Casella, *Eur. J. Inorg. Chem.* **2003**, 3934–3944; c) M. C. Mimmi, M. Gullotti, L. Santagostini, G. Battaini, E. Monzani, R. Pagliarin, G. Zoppellaro, L. Casella, *Dalton Trans.* **2004**, 2192–2201; d) M. Gullotti, L. Santagostini, R. Pagliarin, A. Granata, L. Casella, J. Mol. Catal. A **2005**, *235*, 271–284.

[8] L. Di Bari, G. Pescitelli, P. Salvatori, *J. Am. Chem. Soc.* **1999**, *121*, 7998–8004.

[9] R. B. Kress, E. N. Duesler, M. C. Etter, I. C. Paul, D. Y. Curtin, *J. Am. Chem. Soc.* **1980**, *102*, 7709–7714.

[10] a) L. Casella, M. Gullotti, G. Pallanza, M. Buga, *Inorg. Chem.* **1991**, *30*, 221–227; b) L. Casella, O. Carugo, M. Gullotti, S. Garofani, P. Zanello, *Inorg. Chem.* **1993**, *32*, 2056–2067.

[11] G. Eisenhoffer, I. J. Kopin, D. S. Goldstein, *Pharmacol. Rev.* **2004**, *56*, 331–349.

[12] A. Abragam, B. Bleavey, *Electron Paramagnetic Resonance of Transition Ions*, Claredon Press, Oxford, **1970**.

[13] A. Bencini, D. Gatteschi, *EPR of Exchange Coupled Systems*, Springer, Berlin, **1990**.

[14] P. Comba, Y. D. Lampeka, A. I. Prikhod′ko, G. Rajaraman, *Inorg. Chem.* **2006**, *45*, 3632–3638.

[15] L. Quintanar, J. Yoon, C. P. Aznar, A. E. Palmer, K. K. Andersson, R. D. Britt, E. I. Solomon, *J. Am. Chem. Soc.* **2005**, *127*, 13832–13845.

[16] M. Atanasov, P. Comba, B. Martin, V. Müller, G. Rajaraman, H. Rohwer, S. Wunderlich, *J. Comput. Chem.* **2006**, *27*, 1263–1277.

[17] E. Monzani, L. Quinti, A. Perotti, L. Casella, M. Gullotti, L. Randaccio, S. Geremia, G. Nardin, P. Faleschini, G. Tabbì, *Inorg. Chem.* **1998**, *37*, 553–562.

[18] E. Monzani, L. Casella, G. Zoppellaro, M. Gullotti, R. Pagliarin, R. P. Bonomo, G. Tabbì, G. Nardin, L. Randaccio, *Inorg. Chim. Acta* **1998**, *282*, 180–192.

[19] a) H. J. Prochaska, W. F. Shwindinger, M. Schwartz, M. J. Burk, E. Bernarducci, R. A. Lalancette, J. A. Potenza, H. J. Schugar, *J. Am. Chem. Soc.* **1981**, *103*, 3446–3455; b) J. V. Dagdigian, V. McKee, C. A. Reed, *Inorg. Chem.* **1982**, *21*, 1332–1342.

[20] M. I. Belinsky, *Inorg. Chem.* **2004**, *43*, 739–746.

[21] T. Schewe, Y. Steffen, H. Sies, *Arch. Biochem. Biophys.* **2008**, *476*, 102–106.

[22] E. Monzani, G. Battaini, A. Perotti, L. Casella, M. Gullotti, L. Santagostini, G. Nardin, L. Randaccio, S. Geremia, P. Zanello, G. Opromolla, *Inorg. Chem.* **1999**, *38*, 5359–5369.

[23] A. K. Rappe, C. J. Casewit, K. S. Colwell, W. A. Goddard III, W. M. Skiff, *J. Am. Chem. Soc.* **1992**, *114*, 10024–10035.

[24] M. J. Frisch, G. W. Trucks, H. B. Schlegel, G. E. Scuseria, M. A. Robb, J. R. Cheeseman, J. A. Montgomery Jr., T. Vreven, K. N. Kudin, J. C. Burant, J. M. Millam, S. S. Iyengar, J. Tomasi, V. Barone, B. Mennucci, M. Cossi, G. Scalmani, N. Rega, G. A. Petersson, H. Nakatsuji, M. Hada, M. Ehara, K. Toyota, R. Fukuda, J. Hasegawa, M. Ishida, T. Nakajima, Y. Honda, O. Kitao, H. Nakai, M. Klene, X. Li, J. E. Knox, H. P. Hratchian, J. B. Cross, C. Adamo, J. Jaramillo, R. Gomperts,

R. E. Stratmann, O. Yazyev, A. J. Austin, R. Cammi, C. Pomelli, J. W. Ochterski, P. Y. Ayala, K. Morokuma, G. A. Voth, P. Salvador, J. J. Dannenberg, V. G. Zakrzewski, S. Dapprich, A. D. Daniels, M. C. Strain, O. Farkas, D. K. Malick, A. D. Rabuck, K. Raghavachari, J. B. Foresman, J. V. Ortiz, Q. Cui, A. G. Baboul, S. Clifford, J. Cioslowski, B. B. Stefanov, G. Liu, A. Liashenko, P. Piskorz, I. Komaromi, R. L. Martin, D. J. Fox, T. Keith, M. A. Al-Laham, C. Y. Peng, A. Nanayakkara, M. Challacombe, P. M. W. Gill, B. Johnson, W. Chen, M. W. Wong, C. Gonzalez, J. A. Pople, *Gaussian 03*, Revision A.1, Gaussian, Inc., Pittsburgh, PA, **2003**.

[25] G. Marino, L. Valente, R. A. W. Johnstone, F. Mohammedi-Tabrizi, G. C. Sodini, *J. Chem. Soc., Chem. Commun.* **1972**, 357–358.

[26] a) S. W. Weidman, E. T. Kaiser, *J. Am. Chem. Soc.* **1966**, *88*, 5820–5827; b) J. L. Muñoz, F. García-Molina, R. Varón, J. N. Rodriguez-Lapez, F. García-Cánovas, J. Tudela, *Anal. Biochem.* **2006**, *351*, 128–138.

Received: September 8, 2008
Published Online: December 23, 2008

